Dynamic monitoring of the Paderno iron arch bridge (1889)

Carmelo Gentile and Antonella Saisi
Department of Structural Engineering, Politecnico di Milano, Milan, Italy

ABSTRACT: The paper presents the most relevant results of the experimental modal analysis of the historic iron bridge at Paderno d'Adda (1889). The dynamic tests, representing the first experimental survey carried out on the global characteristics of the bridge since the load reception tests in 1889 and 1892, were performed in operational conditions (i.e. under traffic and wind-induced excitation) between June 2009 and March 2010 and suggested the opportunity of installing a permanent dynamic monitoring system on the bridge with Structural Health Monitoring purposes.

1 INTRODUCTION

The San Michele bridge over the Adda river at Paderno (Fig.1), built between 1887 and 1889 by the Società Nazionale delle Officine di Savigliano (SNOS), is one of the masterpieces of 19^{th} century iron architecture and a symbol of Italian industrial archaeology heritage (Nascè V. et al. 1984). The historic bridge is protected by the Italian Ministry of Cultural Heritage since 1980.

The bridge includes a truss-box metal girder, 266 m long, resting on nine equally spaced bearings. Four of these bearings are supported by a wide trussed arch while the remaining are supported by three metallic piers and by the abutments.

Notwithstanding the poor state of preservation of the structure, significantly damaged by corrosion, the bridge is still used as a combined road and rail bridge, with the top deck of the truss-box girder carrying one lane of alternate road traffic and the bottom deck housing the tracks of a single-line railway. Furthermore, the bridge has not been saved from the increase in road and rail traffic, generally experienced by the infrastructures during the past years. For example, the number of daily train passages (at present 53) were triplicate from the '80s, although with limits in speed and load, and the one-way alternate road traffic flow loads the bridge almost continuously during the day.

Within a systematic surveillance program of the main infrastructures owned by the Province of Lecco – such as the Victory Bridge (Gentile and Gallino 2007) and the new cable-stayed bridge on the Adda river (Gentile 2010) – three different ambient vibration tests were recently carried out on the roadway deck of the Paderno bridge by the Laboratory of Vibrations and Dynamic Monitoring of Structures (VIBLAB) of the Politecnico di Milano. The first test, performed at the end of June 2009, was aimed at investigating the vertical dynamic characteristics (Gentile and Saisi 2010); subsequently, two other tests were carried out to check the variation over time of the previously identified resonant frequencies (September 2009) and to investigate the transverse dynamic behaviour (October 209).

Since the results of the above experimental investigation suggested to set up a Structural Health Monitoring (SHM) program based on the continuous dynamic monitoring (see e.g. Magalhães et al. 2008), a further dynamic test was carried out on March 2010 in collaboration with the Italian Railway Authority; during this test, the acceleration response of the bridge was measured at selected points of both the roadway and the railway deck, with the two-fold objective of better understanding the dynamic characteristics and of optimizing the design and installation of a permanent dynamic monitoring system on the railway deck.

After a description of the historic bridge, full details on the dynamic tests, the experimental procedures, the data analysis techniques and the identified dynamic characteristics (i.e. natural frequencies, mode shapes and damping ratios) are given in the paper. In order to assess the accuracy of the identified modal parameters in view of the future monitoring, the most significant mode shapes and associated natural frequencies were determined by using two complementary output-only identification techniques with different theoretical bases: the

Frequency Domain Decomposition (Brincker R. et al. 2000) and the data-driven *Stochastic Subspace Identification* (SSI, van Overschee and De Moor 1996, developed in the time domain).

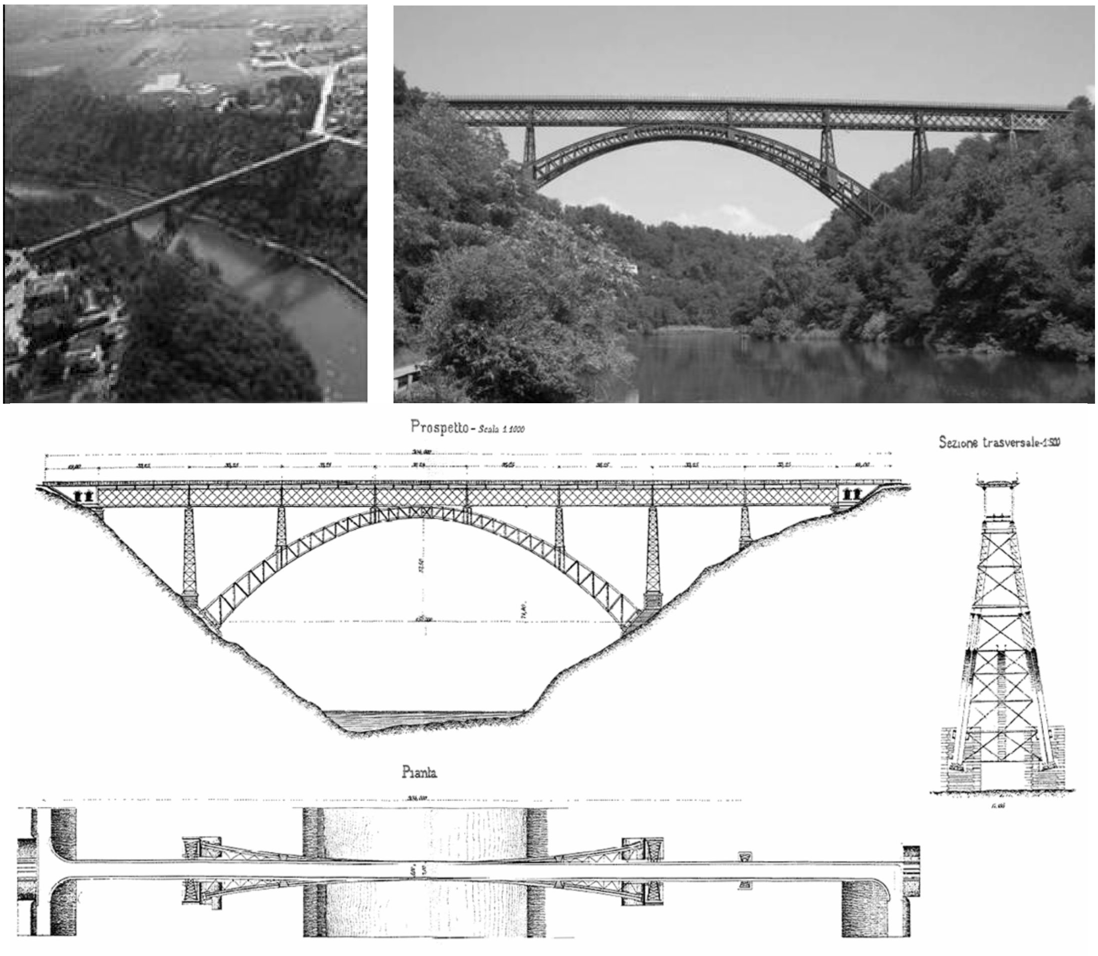

Figure 1 : Views, elevation, plan and cross-section of the iron arch bridge at Paderno d'Adda (1889)

2 DESCRIPTION OF THE BRIDGE AND HISTORIC BACKGROUND

The Paderno Bridge (Fig.1) was designed in 1886 by the head of SNOS technical division, the Swiss engineer Julius Röthlisberger (1851–1911), through the rigorous application of the Theory of the Ellipse of Elasticity (Nascè V. et al. 1984, Ferrari R. and Rizzi E.2008). The project was chosen between four proposals, due to the reduced erection time, only 18 months: the construction officially began on September 1887, with the abutments and the complex scaffolding structure (Fig.2), and was completed on March 1889.

The structural architecture of the bridge and the accurate detailing were highly appreciated so that it was the first Italian bridge to win an international award.

The iron arch bridge (Fig.1-2), crossing the Adda river between Calusco d'Adda and Paderno, links the two provinces of Bergamo and Lecco about 50 km far from Milan. The bridge was quickly erected between 1887 and 1889 to complete one of the first Italian railway lines (the link between Ponte S. Pietro and Seregno) and to comply with the needs of the rapidly growing industrial activities in the Lombardia region at the end of 19th century.

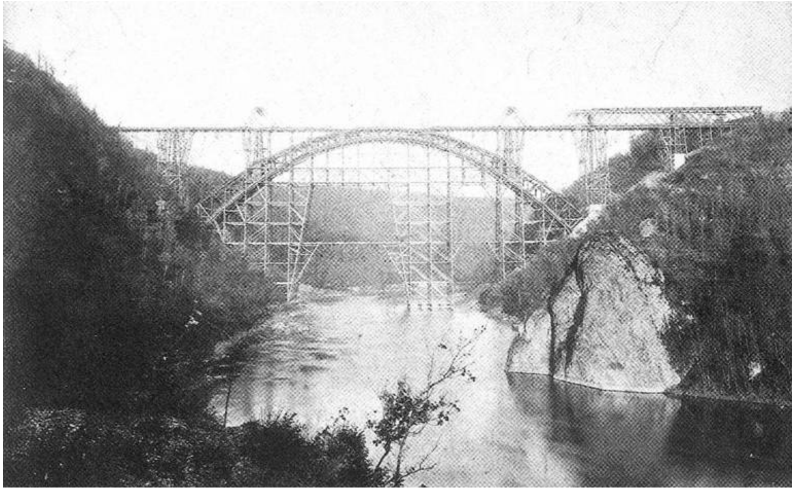

Figure 2 : View of the scaffolding structure and of the iron arch during the bridge construction

(a) (b) (c)

Figure 3 : Structural details of the bridge

The bridge consists of a single span parabolic web arch (Fig.3(a)) and an upper trussed box girder (Fig.3(b)), supported by a series of piers (Fig.3(c)). Three piers are erected from masonry basements while the others are supported by the parabolic arch; all the piers are battered in both directions according to the usual European practice of the late 19^{th} century.

The arch consists of two ribs, with a span of about 150.0 m and rise of 37.5 m; as shown in Fig.3(a), each of the two ribs is composed of double members 1.0 m apart and has a variable height, of between 8.0 m near the supports and 4.0 m at the crown. Since the two parabolic arch ribs are canted inward, the distance between the ribs is variable between 5.0 m at the crown and about 16.35 m at the basements.

The deck is 266.0 m long and comprises 8 spans, supported by 9 equally spaced bearings (33.25 m). The deck vertical trusses, 6.25 m high and 5.0 m apart, consist of with T-shaped section chords connected by multiple lattices (Fig.4) and support two roadways: the upper one (originally with macadam pavement) for roadway and pedestrian traffic, and the lower for a single line of railroad.

The roadway deck, 7.0 m wide and including two walkways, was originally supported by Zorès beams, which were in turn connected to equally spaced (3.325 m) cross-beams. The side walkways, 1.0 m wide, are stone slabs supported by angles connected to the transverse cross-beams (Fig.4(a)).

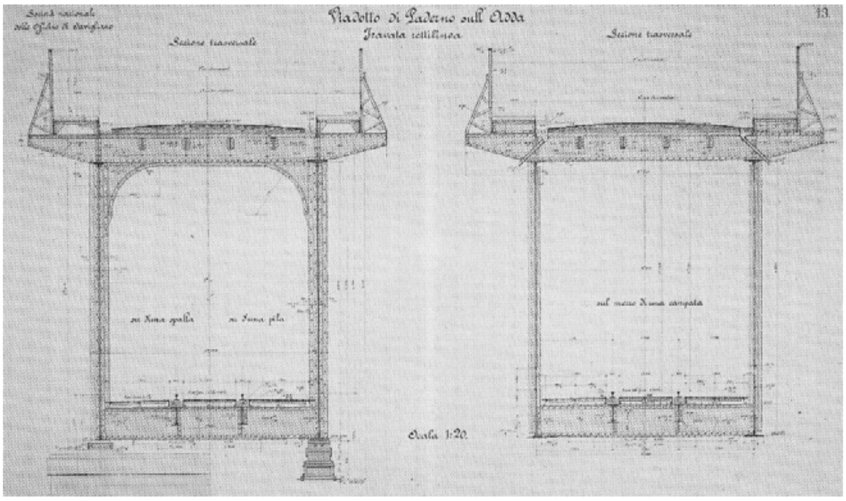

(a)

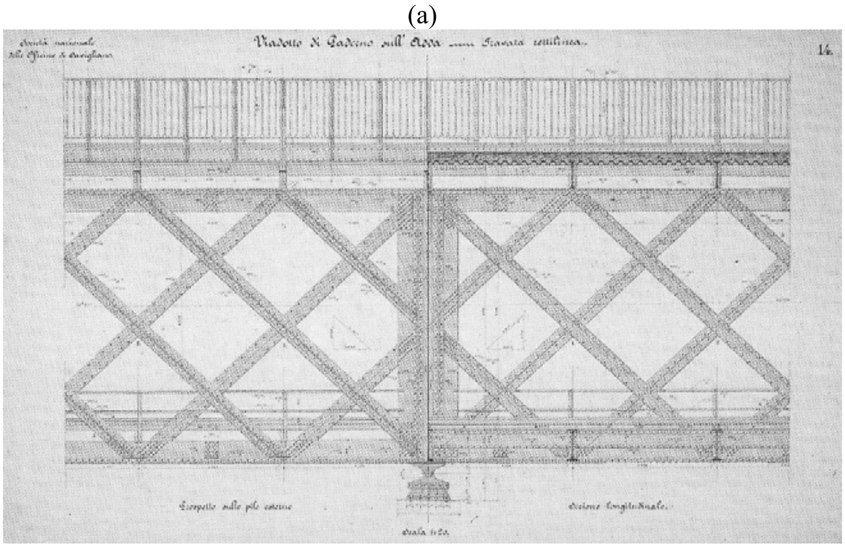

(b)

Figure 4 : Original drawings of : (a) the truss-box girder, (b) the vertical trusses of deck

The railway deck consists of a grid of transverse beams, equally spaced at 3.325 m, and longitudinal beams directly supporting the sleepers, as shown in Fig.4(a).

The piers, shaped like truncated pyramids, are built by 2 truss-box inclined posts, connected by horizontal and bracing elements (Fig.3(c)); each inclined post is composed by 4 angular elements connected by transversal and diagonal members in the 4 main planes.

The basement of the piers and the abutments are built in Moltrasio stone-block masonry and protected by Baveno granite coatings.

The maintenance and inspection procedures were guaranteed by safety passages along the arch axis and by stairs in the piers, nowadays not fully practicable.

All the iron members of the bridge have T or C shaped composite section and are formed by riveted flats and angles.

About 2,600 tons of iron were used in the bridge construction; according to the international classification of Philadelphia (1876), the bridge material can be classified as "wrought iron". Tests carried out on few samples of the bridge members between 1955 and 1972 (see e.g. Nascè et al. 1984) revealed rather poor metallurgical, chemical and mechanical characteristics. As it has to be expected for a wrought iron, the material is characterised by a stratified structure along the rolling plane and frequent non-metallic inclusions, as shown in Fig.5(a); the yield strength is generally larger than 240 MPa, with a tensile strength often less than 300 MPa and rather low (4-12%) elongation. Furthermore, the state of preservation of the bridge is rather poor due to the lack of maintenance; Fig.5(b) exemplifies a typical damage induced by the corrosion, observed on a wide number of structural members: the deformation of the iron plates and sections at the connections of the composite struts, caused by the oxide expansion between the contact plates.

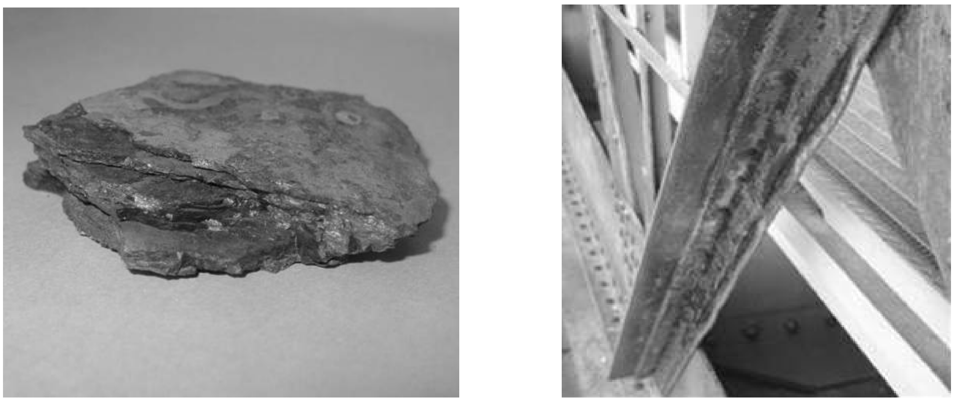

(a) (b)

Figure 5 : (a) Sample of wrought iron coming from the Paderno Bridge, (b) Example of the damage inflicted by the corrosion to the bridge members

The bridge, opened to traffic on May 20th 1889, underwent major modifications and repairs during its history; in particular:

(1) an important retrofit intervention was carried out between 1953 and 1956, aimed at repairing the structural damages suffered during the bomb attacks of the II World War and at re-painting the entire structure;

(2) in 1972, the roadway deck (originally with Zorès beams) was entirely replaced by a steel orthotropic deck connected by rivets to the main structures (Fig.6);

(3) the last intervention dates back to the early '90s and involved mainly the deck (replacement of damaged structural members, stiffening of the trussed box girder, sand-blasting and painting of the structural elements).

Further details of the bridge history and structural characteristics are reported in (Nascè V. et al.1984).

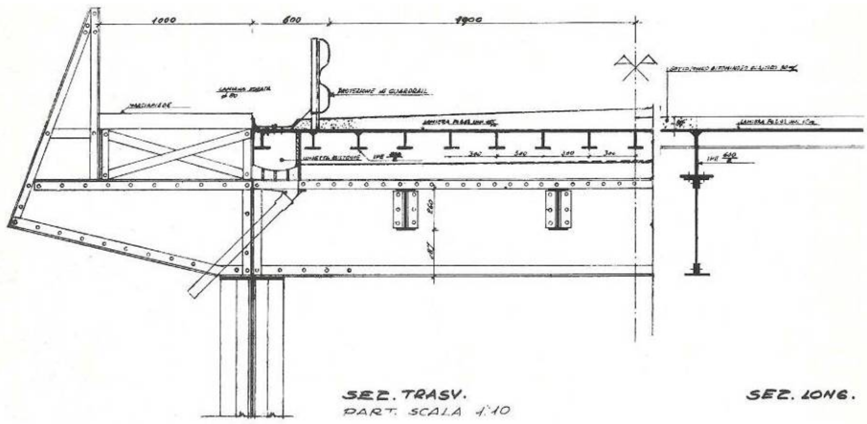

Figure 6 : Structural details of the steel orthotropic plate, that replaced in 1972 the original roadway deck

3 AMBIENT VIBRATION TESTS AND MODAL IDENTIFICATION

After 120 years of use and several structural modifications, and notwithstanding the lack of maintenance and the poor state of preservation of the iron members, the Paderno Bridge is still in service as a combined road and rail bridge.

Since the last experimental investigation of the global behaviour of the structure dates back to the reception load tests performed in 1889 and in 1892, ambient vibration tests (AVT) were carried out between June 2009 and March 2010, with the main objectives of identifying the dynamic characteristics (i.e. natural frequencies, mode shapes and damping ratios) of the bridge and their variation over time. Considering that especially the road traffic causes, together with wind action, permanent and relatively high levels of vibration, AVT is particularly adequate for the identification of modal parameters.

3.1 Experimental procedures

As previously stated, four different AVTs were carried out on the bridge between June 2009 and March 2010; in particular:

(1) the first test, aimed at investigating the vertical modal behavior of the upper girder over the arch, was performed over 2 days (June 29-30, 2009). 2 set-ups were performed to measure the acceleration responses at the opposite sides of 13 cross-sections of the roadway deck, as shown in Fig.7(a), considering 4 sensors (placed at the opposite sides of two reference cross sections) as reference transducers. It should be noticed that the adopted sensor layout cannot provide information on the mode shapes associated with the motion of the part of the upper girder between the arch and the extremity of the bridge on the Calusco side;

(2) the second AVT was carried out on September 22, 2009 by using only two accelerometers (Fig. 7(b)) to check the variation over time of the previously identified resonant frequencies and to investigate the importance of the transverse dynamic behaviour;

(3) as it will be discussed in sect. 4, the spectral analysis of the transverse acceleration recorded in the previous test suggested the existence of a large number of transversal bending modes. Hence, a subsequent AVT was carried out on October 26, 2009, aimed at identifying the transverse modes of vibration and checking again the variation over time of the natural frequencies of the vertical modes. A sketch of the accelerometer layout used in this test is shown in Fig.7(c);

(4) since the results of the previous tests clearly highlighted the effectiveness of the dynamic survey in operation conditions in the SHM of the Paderno Bridge, the Italian Railway Authority (R.F.I.) proposed to VibLab the design of permanent dynamic monitoring system to be placed on the railway deck; the monitoring system would be addressed to real-time identification of possible evolution of the modal parameters indicating the development of anomalies or further damage of the structure and to collect information useful to formulate hypothesis on the future use of the bridge. In order to better understand the modal behaviour and to optimize the number of points on the lower deck to be permanently instrumented, a more extensive campaign of AVT was carried out on March 15-18, 2010. In this last test, both the roadway and the railway deck were simultaneously instrumented, as shown in Fig.7(d) and 7(e); furthermore the vertical and transverse dynamic characteristics were investigated including the previous measurement points (for comparison purposes) on the upper roadway deck but also adding new measurement points on the same deck (Fig.7(a)-(e));

(5) The AVTs were conducted using:

(a) 24-channel data acquisition system, consisting of 6 NI 9234 4-channel dynamic signal acquisition modules (24-bit resolution, 102 dB dynamic range and anti-aliasing filters);

(b) uniaxial WR 731A piezoelectric accelerometers (Fig.7(f)) on the roadway deck; each WR 731A sensor, capable of measuring accelerations of up to ±0.50 g with a sensitivity of 10 V/g, was connected with a short cable (1 m) to a WR P31 power unit/amplifier;

(c) uniaxial WR 799F piezoelectric accelerometers on the railway deck.

3.2 Data processing and operational modal analysis techniques

The modal identification was performed by using the accelerations induced only by the road traffic and at least two time windows of 2500 s were collected in each test and for each sensor layout. Hence, the well-known rule (Cantieni R. 2005) about the length of the time windows acquired (that should be 1000 to 2000 times the period of the structure’s fundamental mode) is largely satisfied.

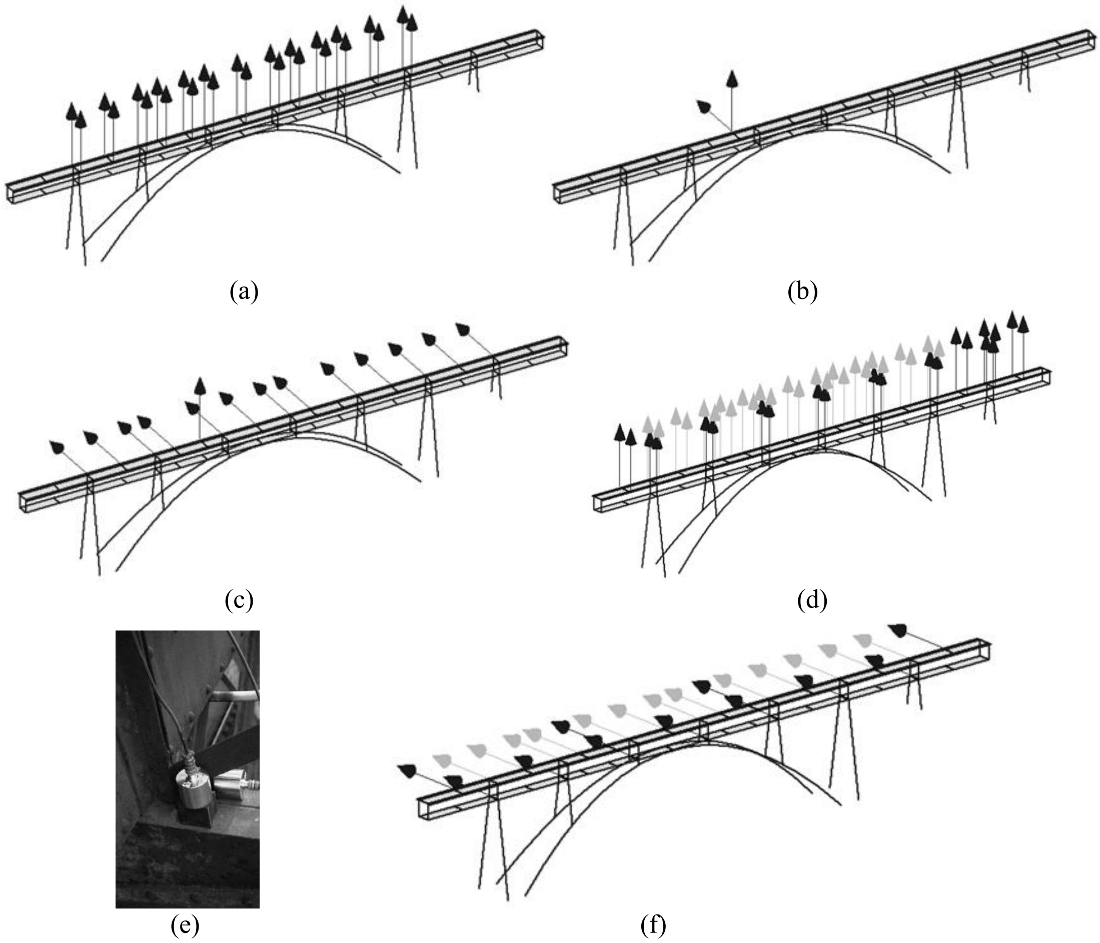

Figure 7 : Measurement points of the ambient vibration tests: (a) June 29-30, 2009; (b) September 22, 2009; (c) October 22, 2009; (d)-(e) March 15-18, 2010. (f) Placement of two accelerometers used

The sampling frequency was 200 Hz, which is much higher than that required for the tested bridge, as the natural frequencies of the dominant modes are below 10 Hz. Hence, a decimation was applied to the data before the use of the identification tools, reducing the sampling frequency from 200 Hz to 12.5 Hz.

The extraction of modal parameters from ambient vibration data was carried out by using frequency domain and the data driven SSI (Van Overschee P. and De Moor B. 1996) in the time domain; these techniques are available in the commercial software ARTeMIS (SVS 2010).

The FDD is based on the evaluation of the spectral matrix (i.e. the matrix of cross-spectral densities):

$$\boldsymbol{G(f)} = \mathbf{E}[\ \boldsymbol{A(f)}\ \boldsymbol{A}^{\mathbf{H}}\boldsymbol{(f)}\ ] \quad (1)$$

where the vector $\boldsymbol{A(f)}$ collects the acceleration responses in the frequency domain, the superscript $^{\mathbf{H}}$ denotes complex conjugate matrix transpose and E denotes expected value. The diagonal terms of the matrix $\boldsymbol{G(f)}$ are the (real valued) auto-spectral densities while the other terms are the (complex) cross-spectral densities. In the present application, the re-sampled time-series were processed in order to estimate $\boldsymbol{G(f)}$ with a frequency resolution of about 0.012 Hz. The FDD technique involves the following steps: (a) evaluation of the spectral matrix $\boldsymbol{G(f)}$; (b) Singular Value Decomposition (SVD) of $\boldsymbol{G(f)}$ at each frequency; (c) inspection of the curves representing the singular values (SV) to identify the resonant frequencies and estimate the corresponding mode shape using the information contained in the singular vectors of the SVD. Since the first (and largest) SV at each frequency represents the strength of the dominating vibration mode at that frequency, plotting the first singular value yields the resonant frequencies as local maxima, as it is shown in Fig.8 and 13 for the investigated bridge.

The SSI method works in the time domain and is based on the discrete-time state-space form of the dynamics of a linear-time-invariant system under unknown excitation:

$$\boldsymbol{x}_{\mathbf{k+1}} = \boldsymbol{B}\ \boldsymbol{x}_{\mathbf{k}} + \boldsymbol{w}_{\mathbf{k}} \tag{2}$$

$$\boldsymbol{y}_{\mathbf{k}} = \boldsymbol{C}\ \boldsymbol{x}_{\mathbf{k}} + \boldsymbol{v}_{\mathbf{k}} \tag{3}$$

where $\boldsymbol{x}_k$ is the discrete-time state vector (containing displacements and velocities describing the state of the system at time instant $t_k = k\Delta t$), $\boldsymbol{w}_{\mathbf{k}}$ is the process noise, $\boldsymbol{y}_{\mathbf{k}}$ is the output vector, $\boldsymbol{v}_{\mathbf{k}}$ is the measurement noise, $\boldsymbol{B}$ is the discrete state matrix (dependent on the mass, stiffness and damping properties of the structure) and $\boldsymbol{C}$ is the discrete output matrix (which maps the state vector into the measured output). Eq. (2) is generally called the state equation while eq. (3) is called the observation/output equation.

It can be shown (Peeters 2000) that the modal parameters (natural frequencies, mode shapes and damping ratios) of a structure under white-noise excitation can be identified by relying only on the measured output responses $\boldsymbol{y}_k$. Once state space matrices are identified of different order *N*, *N/2* modal parameters are extracted from a model of order *N*. If similar modal parameters are obtained with increasing model order, a physical eigenmode is identified. In the present application, stochastic state space models are identified of different order *N*, ranging from 2 to 140-150 in steps of 2.

In order to compare the mode shapes identified using different methods and different test data, the well-known Modal Assurance Criterion (Allemang R.J. and Brown, D.L. 1983) was computed. The MAC value is a coefficient analogous to the correlation coefficient in statistics and ranges from 0 to 1; a value of 1 implies perfect correlation of the two mode shape vectors (one vector is a multiple of the other) while a value close to 0 indicates uncorrelated (orthogonal) vectors. In general, a MAC value greater than 0.85–0.90 is considered a good match while a MAC value less than 0.50 is considered a poor match.

4 DYNAMIC CHARACTERISTICS OF THE PADERNO BRIDGE

4.1 *Vertical bending and torsion modes*

The vertical modes of the bridge, identified in June 2009, are summarized in columns (2)-(4) of Table 1. Eight modes were identified from the SV plot (Fig.8(a)), using the peak-picking technique, and the corresponding mode shapes are shown in Fig.9; all those modes, except the first one, were clearly identified by the SSI method, as well.

Table 1 summarizes the results obtained by applying the FDD and the SSI identification methods through: (a) the natural frequencies (f_{FDD}) identified by the FDD method; (b) the average and the standard deviation values of the natural frequencies ($f_{SSI} \pm \sigma_f$) and modal damping ratios ($\zeta_{SSI} \pm \sigma_\zeta$) identified by the SSI technique. The natural frequencies estimated by the different methods are almost coincident and a similar correspondence was found for most mode shapes (with the MAC value being larger than 0.98), except for the last vertical bending mode VB8; for this mode, the MAC is 0.86 and the FDD technique seems to provide a better estimation of the mode shape.

The modal behavior identified in the first test suggests the following comments:

(1) since the upper deck is loaded by one lane of alternate roadway traffic, with the cars' passages being almost centered, the application of FDD and SSI methods provided the identification of seven vertical bending modes. One torsion mode was identified in the SV plot (Figs. 8-9) only;

(2) although the damping estimates are characterized by large standard deviations for the higher modes, the bridge generally exhibits low values of the damping ratios ($0.3\% < \zeta < 0.8\%$, Table1);

(3) the vertical bending modes are characterized by local violations of the symmetry condition, expected with respect to the vertical plane containing the longitudinal axis of the bridge. The non-symmetric behavior is more clearly identified as the mode order increases. The average difference between the modal deflections on the downstream and upstream sides ranges between 6% (mode VB2) and 24% (mode VB8). It should be noticed that similar shape uneven was not detected in the dynamic assessment of bridges similar to the Paderno Bridge, such as

the Luiz I bridge (1885) over the Douro River in Porto (Calçada R. et al. 2002); hence the mode shapes clearly highlight the different state of preservation of the structural elements on the downstream and upstream sides.

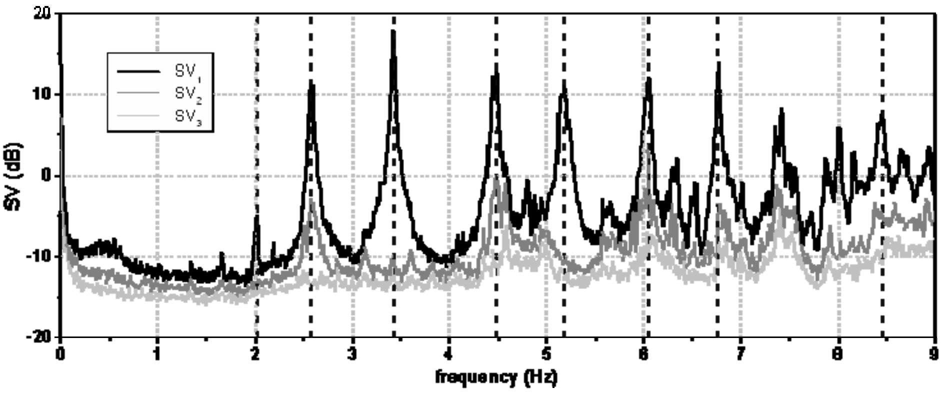

(a)

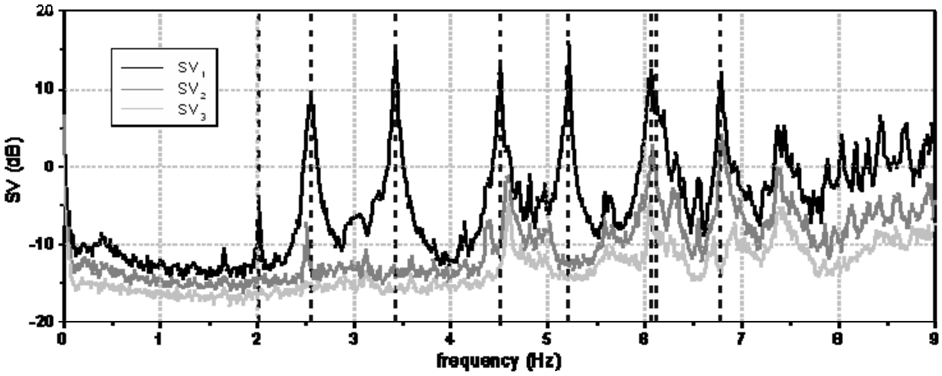

(b)

Figure 8 : Singular value curves and peak picking identification of natural frequencies (FDD): (a) June 29-30, 2009; (b) March 15-18, 2010

Table 1 : Summary of the vertical bending and torsion modes identified by FDD and SSI methods.

Mode	June 2009			March 2010		
	FDD	SSI		FDD	SSI	
Type(*)	f_{FDD} (Hz)	$f_{SSI} \pm \sigma_f$ (Hz)	$\zeta_{SSI} \pm \sigma_\zeta$ (%)	f_{FDD} (Hz)	$f_{SSI} \pm \sigma_f$ (Hz)	$\zeta_{SSI} \pm \sigma_\zeta$ (%)
T1	2.014	–	–	2.014	–	–
VB1	2.582	2.579 ± 0.006	0.67 ± 0.056	2.551	2.553 ± 0.014	0.98 ± 0.332
VB2	3.424	3.418 ± 0.003	0.39 ± 0.038	3.418	3.420 ± 0.008	0.54 ± 0.247
VB3	4.462	4.464 ± 0.013	0.50 ± 0.098	4.498	4.500 ± 0.009	0.49 ± 0.208
VB4	5.176	5.175 ± 0.002	0.51 ± 0.030	5.206	5.204 ± 0.002	0.36 ± 0.133
VB5	6.055	6.046 ± 0.012	0.43 ± 0.199	6.061	6.054 ± 0.009	0.42 ± 0.139
VB6	–	–	–	6.110	–	–
VB7	6.769	6.764 ± 0.008	0.30 ± 0.131	6.787	6.783 ± 0.007	0.35 ± 0.126
VB8	8.453	8.420 ± 0.061	0.79 ± 0.402	–	–	0.79 ± 0.402

*VB: Vertical Bending; T: Torsion

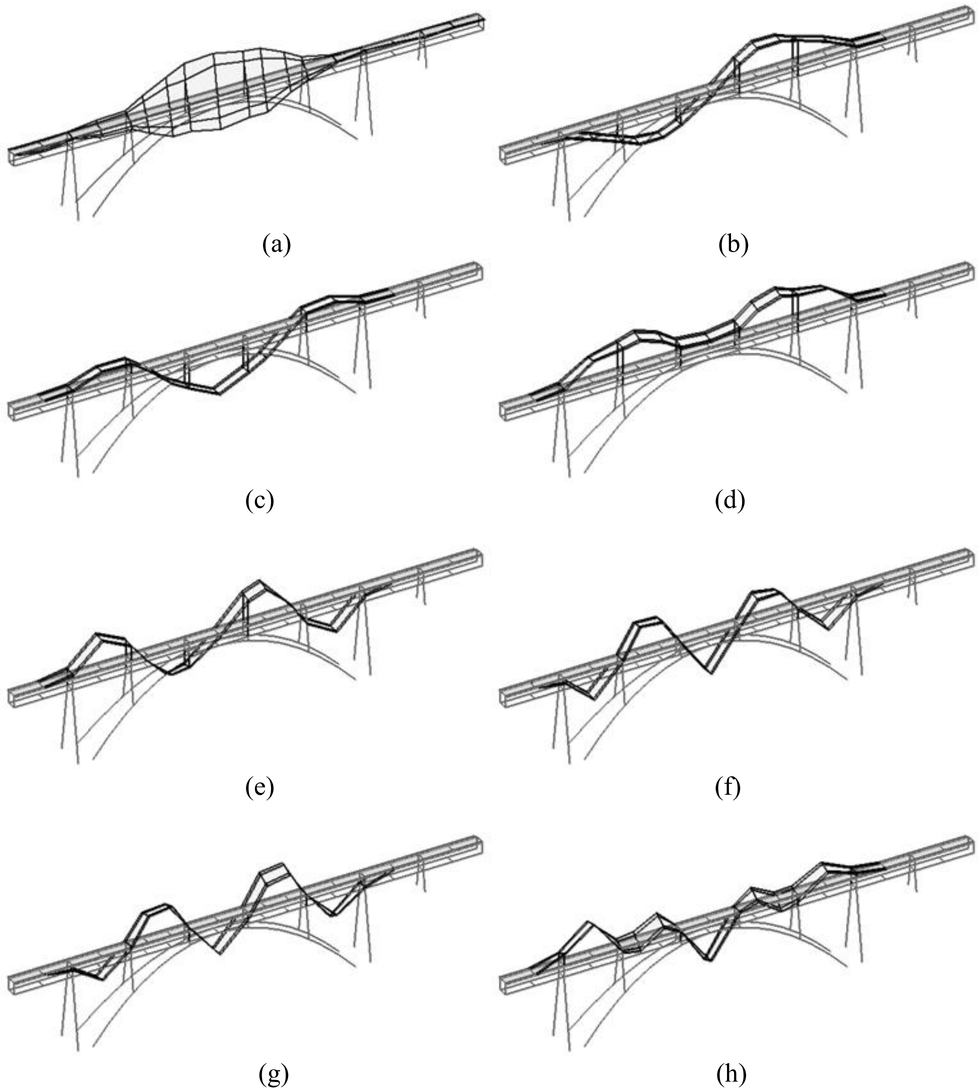

Figure 9 Identified vertical bending and torsion mode shapes (FDD, June 2009): (a) T1: f_{FDD} = 2.01 Hz, (b) VB1: f_{FDD} = 2.58 Hz, (c) VB2: f_{FDD} = 3.42 Hz, (d) VB3: f_{FDD} = 4.46 Hz, (e) VB4: f_{FDD} = 5.18 Hz, (f) VB5: f_{FDD} = 6.06 Hz, (g) VB7: f_{FDD} = 6.77 Hz, (h) VB8: f_{FDD} = 8.45 Hz

Furthermore, the autospectra of the vertical accelerations acquired on June 29th and June 30th reveals slight variations of the natural frequencies. These variations are quite clear in the time-frequency plot of Fig.10(a), which refers to the vertical channel common to all tests (Fig.7), and provided strong motivations for the subsequent experimental checks. Fig.10(b) refers to the September test and shows that, although the variation of the signal frequency content over time seems to be less significant than in Fig. 10(a) (probably as a consequence of lighter traffic flow), the resonant frequency of the first vertical bending mode decreased with respect to the previous test. Although no further variation was observed in the tests of October 2009 and March 2010, as shown iin Fig.10(c) and 10(d), the experimental evidence of slight non-linearity and possible increase of damage (decrease of the natural frequency of the first bending mode) suggested the opportunity of installing a permanent dynamic monitoring system on the bridge with SHM purposes.

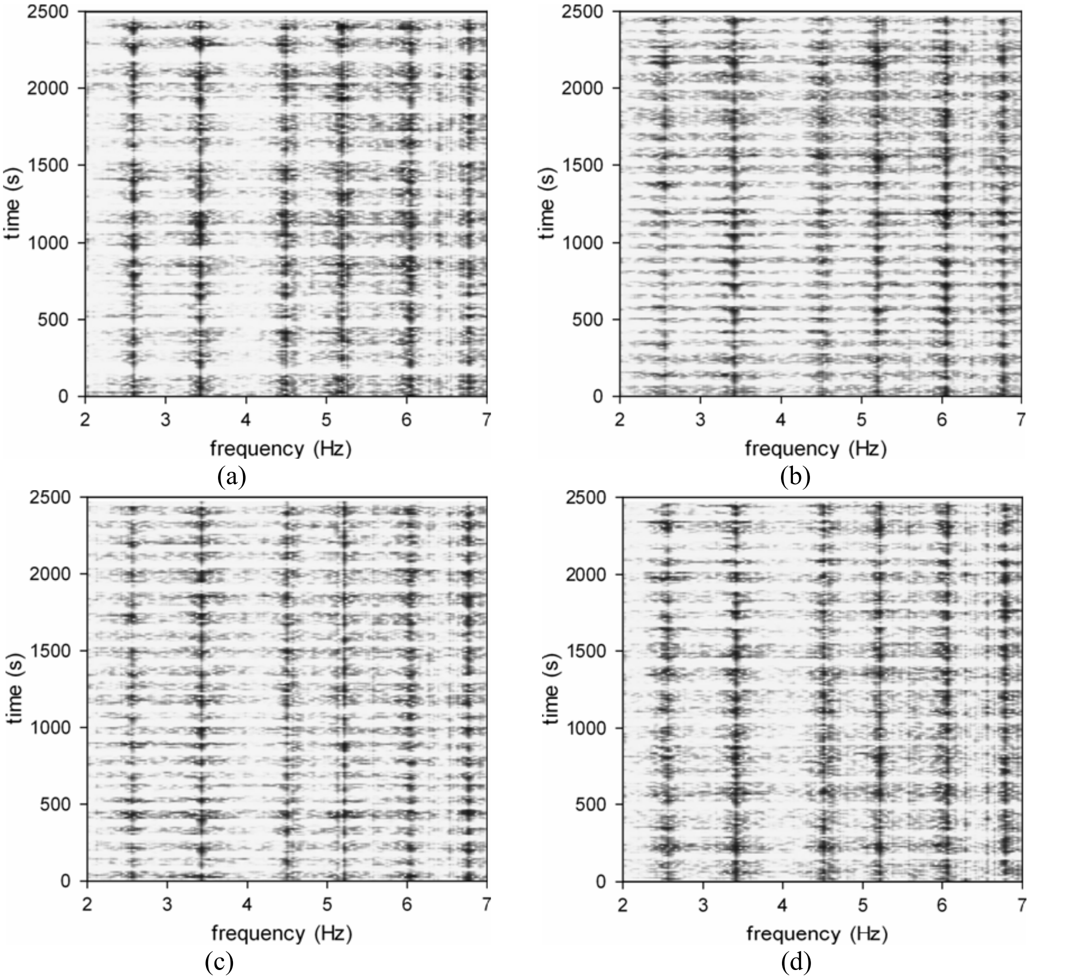

Figure 10: Time-frequency plots with the variation of the signal frequency content over time: (a) June 29th, 2009, (b) September 22nd, 2009, (c) October 26th, 2009, (d) March 18th, 2010

The results in terms of vertical modes obtained in the March 2010 test are summarized in columns (5)-(7) of Table 1. With respect to the June 2009 test, a further vertical bending mode was identified (Fig.8(b)); this mode, referred to as VB6 in Table 1 and shown in Fig.11, mainly involves the motion of the upper girder between the arch and the extremity of the bridge on the Calusco side. The test results also revealed that modes VB5 and VB7 are characterized by the dominant motion of the upper roadway deck with respect to the railway one.

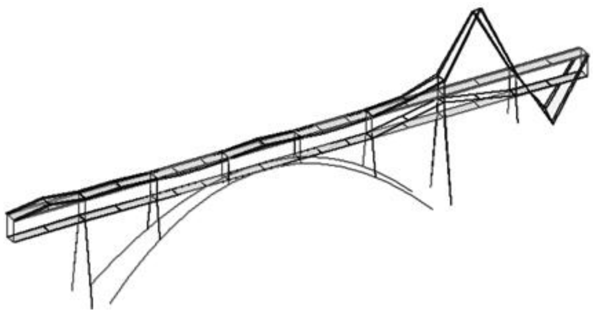

Figure 11 : Vertical bending mode VB6 identified in March 2010 test (FDD)

Furthermore, the inspection of the SV plots of Fig.8(a) and 8(b) – which refer to the two tests performed on June 2009 and Marc/h 2010, respectively – highlights that the two curves of the first singular value are very similar between the two tests, with the main difference being related to: (a) the decrease of the natural frequency of the first vertical bending modes and (b) the spectral peak at 6.11 Hz in Fig.8(b), corresponding to mode VB6. Although the correspondence between the modal deflections in measurement points common to the two tests is very good (Fig.12), it has to be observed that the MAC values are 0.952 and 0.959 for modes T1 and VB7, respectively; hence, slight variation of these mode shapes is suggested between the two tests.

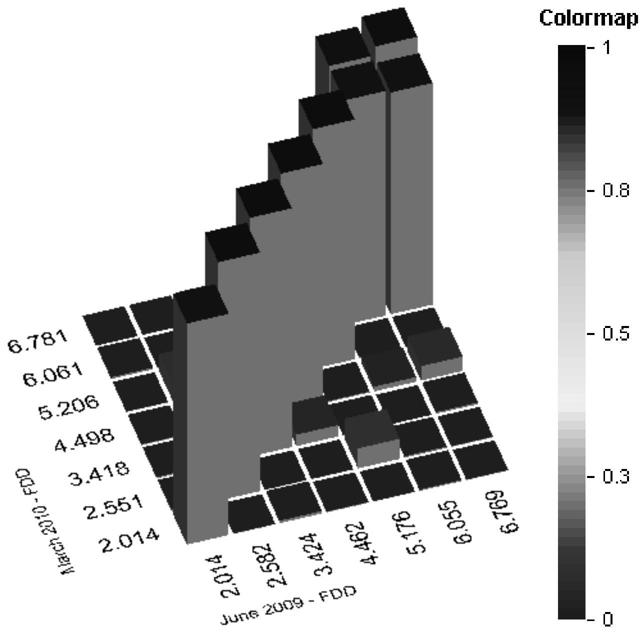

Figure 12 : MAC matrix between the vertical modes identified on June 2009 and on March 2010 (FDD)

4.2 *Transversal bending modes*

The results of the operational modal analysis in terms of natural frequencies of the transversal bending modes are summarized through the spectral plots of Fig.13(a) and 13(b); these figures show the averages of the first 3 normalized Singular Values of the spectral matrices of all data sets recorded in the two tests of October 2009 and March 2010, respectively. The inspection of Figs.13(a) and 13(b) yields to the identification of 17 normal modes in the frequency interval (0–6 Hz) and clearly highlights the correspondence of the natural frequencies between the two different AVTs, with the local maxima of Fig.13(a) (October 2009) being placed practically at the same frequencies of those in Fig.13(b) (March 2010). The two curves of the first singular value are also very similar between the two tests, with the main difference being related to the spectral peaks corresponding to modes TB11 and TB15, that are more clear in Fig.13(a).

All the transverse modes identified by applying the FDD technique to the data collected in the first AVT were clearly identified by the SSI method, as well. The data recorded on March 2010 provided quite clear identification of the modes TB11 and TB15 by using the FDD technique only. Table 2 summarizes the results obtained by applying the FDD and the SSI identification methods through: (a) the natural frequencies (f_{FDD}) identified by the FDD method; (b) the average and the standard deviation values of the natural frequencies ($f_{SSI} \pm \sigma_f$) and modal damping ratios ($\zeta_{SSI} \pm \sigma_\zeta$) identified by the SSI technique.

The natural frequencies estimated by the different methods in the two tests are practically coincident and a similar correspondence was found for the mode shapes (again, with the exception of modes TB11 and TB15, that were less clearly excited in the last test).

Furthermore, the inspection of the standard deviation values in Table 2 reveals not only very low scatter of the natural frequency estimates but also low values of σ_ζ, especially for the data collected on October 2009, when an unique sensors' set-up was adopted.

Table 2: Summary of the transversal bending (TB) modes identified by FDD and SSI methods.

Mode	October 2009			March 2010		
	FDD	SSI		FDD	SSI	
Type	f_{FDD} (Hz)	$f_{SSI} \pm \sigma_f$ (Hz)	$\zeta_{SSI} \pm \sigma_\zeta$ (%)	f_{FDD} (Hz)	$f_{SSI} \pm \sigma_f$ (Hz)	$\zeta_{SSI} \pm \sigma_\zeta$ (%)
TB1	0.989	0.986 ± 0.000	0.41 ± 0.011	0.989	0.988 ± 0.000	0.45 ± 0.025
TB2	1.343	1.338 ± 0.001	0.69 ± 0.103	1.343	1.339 ± 0.001	0.76 ± 0.096
TB3	1.648	1.646 ± 0.000	0.57 ± 0.053	1.648	1.648 ± 0.002	1.03 ± 0.514
TB4	2.008	2.005 ± 0.000	0.53 ± 0.011	2.014	2.015 ± 0.007	0.82 ± 0.290
TB5	2.179	2.176 ± 0.001	0.77 ± 0.066	2.185	2.179 ± 0.003	0.79 ± 0.160
TB6	2.509	2.511 ± 0.001	0.57 ± 0.031	2.509	2.512 ± 0.003	0.54 ± 0.078
TB7	2.832	2.831 ± 0.003	0.56 ± 0.135	2.832	2.836 ± 0.002	0.60 ± 0.140
TB8	3.119	3.109 ± 0.001	0.59 ± 0.054	3.119	3.118 ± 0.004	0.64 ± 0.106
TB9	3.577	3.580 ± 0.005	0.98 ± 0.223	3.589	3.591 ± 0.006	0.60 ± 0.087
TB10	3.802	3.798 ± 0.003	0.59 ± 0.020	3.815	3.835 ± 0.048	1.23 ± 1.382
TB11	4.059	4.076 ± 0.002	0.82 ± 0.018	4.083	–	–
TB12	4.144	4.130 ± 0.002	0.78 ± 0.009	4.132	4.150 ± 0.005	0.63 ± 0.500
TB13	4.376	4.370 ± 0.003	0.50 ± 0.064	4.382	4.377 ± 0.009	0.30 ± 0.148
TB14	4.565	5.563 ± 0.001	0.59 ± 0.055	4.572	4.567 ± 0.002	0.66 ± 0.273
TB15	4.785	4.789 ± 0.005	0.82 ± 0.057	4.810	–	–
TB16	4.932	4.932 ± 0.003	0.86 ± 0.033	4.962	4.956 ± 0.012	0.85 ± 0.125
TB17	5.591	5.575 ± 0.001	1.21 ± 0.013	5.609	5.618 ± 0.007	1.01 ± 0.025

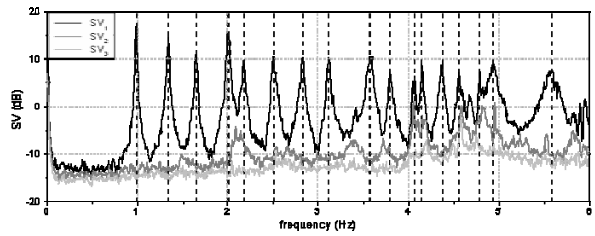

(a)

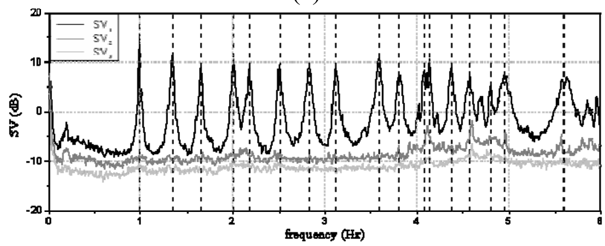

(b)

Figure 13 : Singular value curves and peak picking identification of natural frequencies (FDD): (a) October 26, 2009; (b) March 15-18, 2010

The availability of measurement points on both decks of the girder, in the test carried out on March 2010, provided valuable information on the relative transverse motion between the roadway and the railway deck and hence, on the transversal deformability of the truss-box girder. The transversal bending modes identified during this test (FDD technique) are represented in Fig.14 and the inspection of the mode shapes clearly shows that, as the mode order increases, the two decks exhibit significant relative (and even out-of-phase) transverse motion.

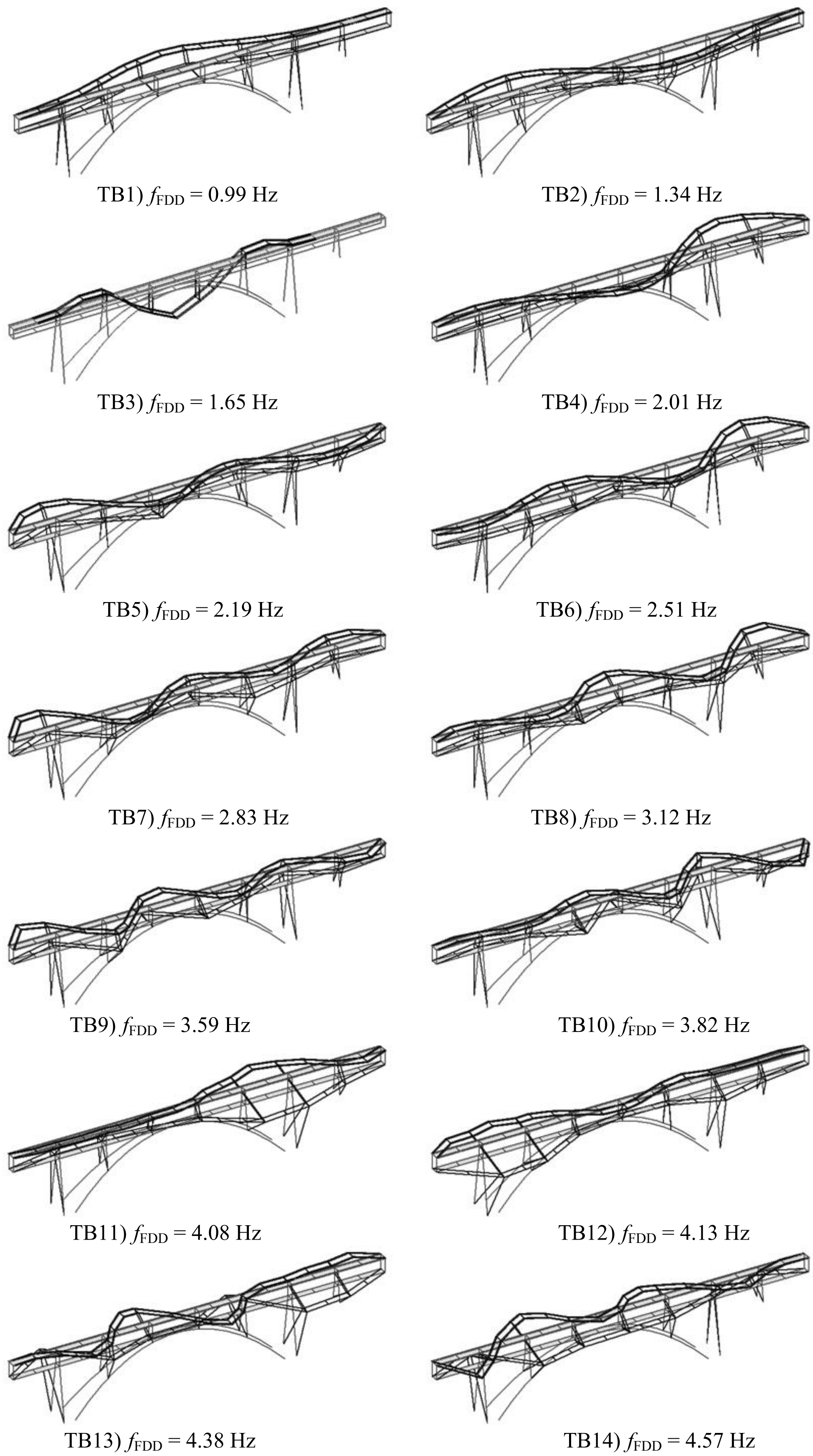

TB1) f_{FDD} = 0.99 Hz TB2) f_{FDD} = 1.34 Hz

TB3) f_{FDD} = 1.65 Hz TB4) f_{FDD} = 2.01 Hz

TB5) f_{FDD} = 2.19 Hz TB6) f_{FDD} = 2.51 Hz

TB7) f_{FDD} = 2.83 Hz TB8) f_{FDD} = 3.12 Hz

TB9) f_{FDD} = 3.59 Hz TB10) f_{FDD} = 3.82 Hz

TB11) f_{FDD} = 4.08 Hz TB12) f_{FDD} = 4.13 Hz

TB13) f_{FDD} = 4.38 Hz TB14) f_{FDD} = 4.57 Hz

Figure 14 : Identified transversal bending mode shapes (FDD, March 2010)

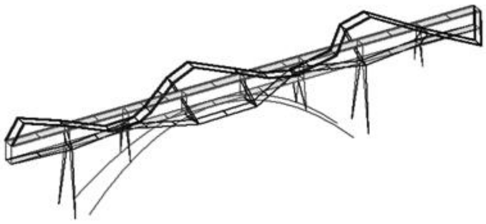

TB15) f_{FDD} = 4.81 Hz

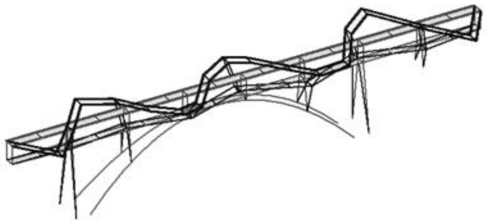

TB16) f_{FDD} = 4.96 Hz

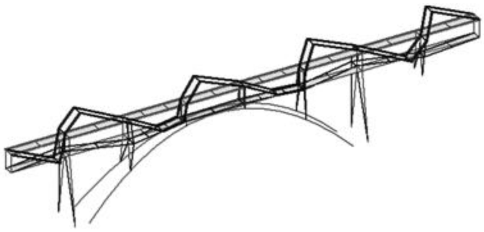

TB17) f_{FDD} = 5.61 Hz

Figure 15 : (cont'd): Identified transversal bending mode shapes (FDD, March 2010)

5 CONCLUSIONS

The paper focuses on the operational modal analysis of the historic San Michele Bridge (1889) over the Adda river. Four different dynamic tests were performed in operational conditions on the iron arch bridge, between June 2009 and March 2010.

The most significant mode shapes and associated natural frequencies were determined in the frequency range 0–10 Hz, by using the FDD and SSI output-only identification techniques, in order to assess the accuracy of the identified modal parameters. The ambient vibration tests allowed the identification of 17 transversal bending modes and 9 vertical bending or torsion modes in the investigated frequency range. Furthermore, an excellent agreement was generally found between the modal estimates obtained from the FDD and SSI techniques in each series of tests.

Based on the identified modal behaviour and their variation over time, the following conclusions can be drawn:

(1) the natural frequencies of the vertical bending modes generally exhibit slight variations over time, possibly depending on the excitation/response level;

(2) the vertical bending modes are non-symmetric with respect to the vertical plane containing the longitudinal axis of the bridge, clearly indicating the different state of preservation of the structural iron members on the downstream and upstream sides;

(3) the resonant frequency of the first bending mode slightly decreased after the first AVT, carried out on June 29-30, 2009;

(4) few vertical modes seem to exhibit variation between the two tests of June 2009 and March 2010;

(5) although the dynamic characteristics in the transverse direction seem time-invariant, the mode shapes clearly reveal an excessive transversal deformability of the truss-box girder, with the two decks exhibiting significant (and even out-of-phase) relative motion in the transverse direction.

As a consequence, permanent dynamic monitoring has to be considered mandatory to accurately survey the possible evolution of the actual bridge condition. The SHM system has been already designed (based on Kistler and NI components) by VIBLAB and will be installed on the railway deck as soon as possible.

6 ACKNOWLEDGEMENTS

The research was supported by the Province of Lecco. The authors would like to thank PhD N. Gallino, M. Antico, M. Cucchi (VIBLAB, Laboratory of Vibrations and Dynamic Monitoring of Structures, Politecnico di Milano) and CE M. Campostrini (R.F.I., Italian Railway Authority) for the assistance during the field tests. Furthermore, the valuable help of CE F. Busatta (in the analysis of the data acquired on March 2010), Kistler Italia and NI (in the design of the SHM system) are gratefully acknowledged.

REFERENCES

Allemang R.J. and Brown, D.L. 1983. Correlation coefficient for modal vector analysis, Proc, 1st Int. Modal Analysis Conference (IMAC), p.110-116.

Brincker R., Zhang L.M. and Andersen P., 2000. Modal identification from ambient responses using Frequency Domain Decomposition, Proc, 18th Int. Modal Analysis Conference (IMAC), p.625-630.

Calçada R., Cunha A. and Delgado R. 2002. Dynamic analysis of metallic arch railway bridge, J. Bridge Engineering ASCE, **7**(4), p.214-222.

Cantieni R., 2005. Experimental methods used in system identification of civil engineering structures, Proc, 1st Int. Operational Modal Analysis Conf, (IOMAC'05), p.249-260.

Ferrari R. and Rizzi E., 2008. On the theory of the ellipse of elasticity as a natural discretisation method in the design of Paderno d'Adda Bridge (Italy), Proc, SAHC 2008, p.583-591.

Gentile C. and Gallino N., 2007. Ambient vibration-based investigation of the "Victory" arch bridge, Proc, 5th Int. Conference on Arch Bridges (ARCH'07), p.63-70.

Gentile C., 2010. Deflection measurement on vibrating stay cables by non-contact microwave interferometer, NDT&E International, 43(3), p.231-240.

Gentile C. and Saisi A., 2010. Dynamic assessment of the iron bridge at Paderno d'Adda (1889), Proc, SAHC 2010 (in press).

Magalhães F., Cunha, A. and Caetano E., 2008. Dynamic monitoring of a long span arch bridge, Engineering Structures, 30(11), p.3034-3044.

Nascè V., Zorgno A.M., Bertolini C., Carbone V.I., Pistone G. and Roccati R. 1984, Il ponte di Paderno: storia e struttura, Conservazione dell'architettura in ferro, Restauro, p.73-74

Peeters B., 2000. System identification and damage detection in civil engineering structures, Ph.D. Thesis, Heverlee, Belgium: Katholieke Universiteit Leuven.

Peeters B. and De Roeck G., 1999. Reference-based stochastic subspace identification for output-only modal analysis. Mechanical Systems and Signal Processing, 6(3), p.855-878.

Società Nazionale delle Officine di Savigliano, 1889. Il viadotto di Paderno sull'Adda (ferrovia Ponte S. Pietro-Seregno), Camilla e Bertolero, Torino.

SVS 2010. ARTeMIS Extractor 2010 release 5.0., http://www.svibs.com/.

Van Overschee P. and De Moor B., 1996. Subspace identification for linear systems: Theory, implementation, applications, Kluwer Academic Publishers.